



# Drainage morphometry and groundwater potential mapping: application of geoinformatics with frequency ratio and influencing factor approaches

Arjun Doke<sup>1</sup> · Sudhakar D. Pardeshi<sup>2</sup> · Sumit Das<sup>2</sup>

Received: 6 October 2017 / Accepted: 10 August 2020 / Published online: 17 August 2020  
© Springer-Verlag GmbH Germany, part of Springer Nature 2020

## Abstract

Morphometric analyses have the ability to provide substantial evidences of drainage evolution, hydro-geomorphic, denudation, and tectonic characteristics that are essential for sustainable watershed management and planning. The aim of this study is to investigate different morphometric parameters and groundwater potentials in Savitri and Vashisthi basins through geographic information system (GIS) techniques. Utilizing high-resolution satellite images, conventional datasets, and relevant field data, we prepared eight thematic layers that regulate the groundwater potentials of an area, such as geology, lineaments, drainage density, slope, rainfall, soil texture and depth, and well density. All these conditioning factors were analyzed in GIS using weighted sum method utilizing the influencing factor (IF) and frequency ratio (FR) methods to prepare the groundwater potential maps. The resultant groundwater potential maps were classified into four sections of different potentiality as: very high, high, moderate, and low. The accuracy of these groundwater potential maps was confirmed by area under the curve (AUC) through establishing a relationship between cumulative percentage of different groundwater potential classes and cumulative percentage of the availability of wells. Prediction of groundwater potentials through FR showed pronounced efficiency (AUC = 75%) for both drainage basins compared to the IF technique (AUC = 69% and 65% for Savitri and Vashisthi, respectively). It was summarized that the reliability of FR technique is higher, contrasting to the IF technique for groundwater potential mapping in our study area. Moreover, morphometric parameters indicated that the drainage development is highly mature in both catchments. The resultant groundwater potential maps can be used for sustainable water resource management and developing artificial recharge projects in the study area.

**Keywords** Morphometric analysis · Groundwater potential · Frequency ratio · Influence factor · GIS · India

## Introduction

Groundwater is an essential natural resource that has a significant influence on biospheric, geospheric, and atmospheric processes. However, without water, no living being can stay alive for a long time, except few microbes and bacteria. About two-third of the earth's surface is covered by oceans, which contain a huge volume of water, but still there is a severe water resource scarcity because of the

limited accessibility of fresh water. Glacier melts, subsurface water, and the rivers are the only source of fresh water, which can be consumed in domestic and economic activities (Das et al. 2017). Since the early twentieth century, the population growth is very high in a few developing countries such as China, India, Brazil, etc. Due to the over-population growth, the consumption rate of water is extremely high due to intensive agricultural and industrial practices. As a result, the reservoirs in these countries are depleting rapidly and regions are becoming more vulnerable to drought (Das 2019a). Therefore, these regions are required to have proper watershed management and groundwater resource planning to prevent water resource scarcity.

Management of watersheds, available natural resources, and assessment of groundwater can easily be done through morphometric analysis. The surface characteristics, geomorphic landforms, and underlying geological structures

✉ Sumit Das  
sumit.das.earthscience@gmail.com

<sup>1</sup> Department of Geography, Baburaoji Gholap College, Pune 411027, India

<sup>2</sup> Department of Geography, Savitribai Phule Pune University, Pune 411007, India

with their characteristics the region's topographic information can be described through drainage basin morphometry (Das et al. 2018). Groundwater occurrence, movement, and storage in an area are controlled by the geological and geomorphological setup of the area. There is a direct and indirect influence of geological and geomorphological factors on the hydrological settings of an area. At the same time, the amount of runoff, infiltration, and rate of percolation are governed through the physiographic elements such as relief and slope (Das 2019b).

Numerous researchers performed studies on the morphometric analysis of different basins through conventional methods (Horton 1945; Smith 1950; Strahler 1957). Morphometric analysis is comprehensively utilized for integrated land and water resources management, and identification of groundwater potential zones (Mishra et al. 2011; Das and Pardeshi 2018a). The morphometric analysis assisted for identification of suitable sites for the construction of artificial recharge dams (Zaidi 2011).

Until late twentieth century, drainage basin analysis used to be done using traditional techniques such as topographic map analysis and aerial photograph interpretation. However, innovation of GIS made the geo-environmental assessments easier than ever (Ghasempunia and Herfeh 2017; Das 2019c). Digital elevation model (DEM) coupled with GIS software is an easy, time and money-effective tool for various geological and geomorphological applications such as drainage basin analysis, extraction of lineaments, geo-environmental modelling (Farr and Kobrick 2000; Grohmann 2004; Sreedevi et al. 2009; Benffai et al. 2017). Many multi-criteria decision techniques have been used by previous workers through GIS platform for the assessment of groundwater, for example, analytical hierarchy process, fuzzy logic, weighted overlay analysis etc. (Hosseini and Saremi 2018).

The Central Groundwater Board of India (CGWB 2012) estimated that the annual replenishable water resource in the country is about 431 km<sup>3</sup>. States like Rajasthan, Gujrat, Maharashtra, Panjub, and Haryana are being depleted since last few decades (Rodell et al. 2009). Savitri and Vashisthi basins are located in the central part of coastal Maharashtra, where a severe water resource scarcity occurs during the summer. These two basins contribute a large area of agricultural land which require a constant supply of water throughout the entire year. Hence, water resource management and identification groundwater potential zones are critical requirements in these regions. Hence, an attempt has been made in this study to evaluate the morphometric analysis and groundwater potential zonation of Savitri and Vashisthi basin through geospatial analysis. Besides mapping of groundwater potential zones, the aim of our work was extended to compare two popular methods (frequency ratio and influencing factor) that are widely used for groundwater potential mapping.

## Study area

Savitri and Vashisthi catchments are located at the base of the Western Ghat escarpment, encompassing an area of 2262 and 2163 km<sup>2</sup>, respectively, (Fig. 1). All the streams within Savitri and Vashisthi basins are originating from escarpment of the Western Ghat, flowing westward and falling into the Arabian Sea. A large part of both basins are covered by dispersed vegetation. Very steep slope characterises the upstream section of both catchments. Dendritic drainage pattern is the primary drainage arrangement followed by parallel and rectangular in the study area. Vashisthi shows numerous small water bodies such as lakes, dams, etc. The topographic slope is towards the west and many isolated hills can be observed in both basins.

The major lithology is basalt in both catchments. Laterites can be found at a different elevation (0–1400 m) with a flat to undulating topography (Widdowson and Cox 1996). The thickness of the laterite is highly variable from the coastal region to the escarpment. Savitri and Vashisthi basins show numerous dykes having an orientation with NNE–SSW direction (Das and Pardeshi 2018b). The entire study area can be categorised into three prominent geomorphic divisions: (1) very steep escarpment in the eastern part from where all the streams are originating; (2) the gentle pediment with scattered hills in the central part; and (3) the lowland coastal region.

The study area shows monsoon climatic condition where the rainfall intensity is very high in the monsoon season (June–Sept). The average annual rainfall in the study area is about 3000 mm (Doke et al. 2018). Though substantial rainfall occurs during monsoon, the summer period experiences drought like conditions in both catchments.

## Methodology

In this study, we performed drainage morphometry and groundwater potential mapping using geospatial techniques. We obtained Shuttle Radar Topographic Mission (SRTM) DEM from <https://srtm.csi.cgiar.org/>. Initially, we processed the DEM in ArcGIS 10.1 software and projected to WGS 1984 UTM 43N coordinate system. After that, we performed flow direction, flow accumulation, and basin tools to generate the basin raster. Subsequently, basin rasters were converted into vector format, and Savitri and Vashisthi basin DEMs were extracted using those basin vector files. After this procedure, the methodology was divided into four sections for morphometric analysis, extraction of lineaments, digitization of different thematic layers, and demarcation of groundwater potential zones.

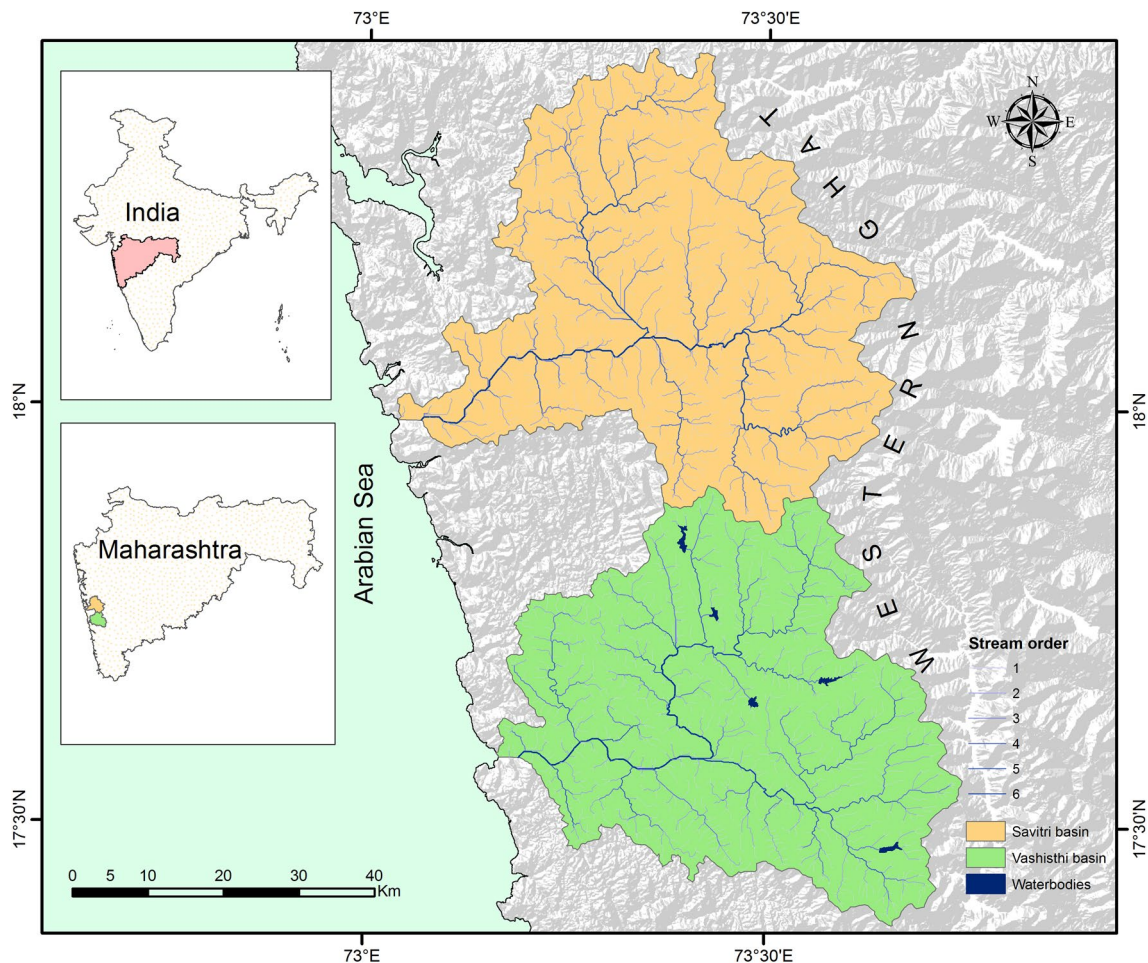


**Fig. 1** Location map of the study area referenced to India and Maharashtra state. Savitri and Vashisthi are classified as sixth-order drainage basin

## Morphometric analysis

We used filled DEM to create flow direction, flow accumulation, and stream order maps in ArcGIS. Afterward, the data were exported in the Microsoft Excel software and all the essential morphometric parameters were calculated. Table 1 is providing the list of morphometric parameters that we selected for this study with corresponding formulae.

## Extraction of lineament

We extracted lineaments from the shaded relief map. To prepare shaded relief map, SRTM DEM was used in ArcGIS. Das et al. (2018) demonstrated that the accuracy of extraction of the lineaments from shaded relief map depends on the sun elevation angle. Few certain angles are excellent for accurate extraction whereas few creates false topographic perception phenomena (FTPP) (Das et al. 2018). Therefore, the extraction was done on the basis of four different azimuth angles at 90° interval. Digitization of all the geology

and geomorphic surface features (for example cliffs, faults, dykes, straight valleys, etc.) was done manually. Consequently, all these surface features created from different azimuth were merged into a single shapefile. Landsat images and Google Earth were utilized to remove the redundant feature and the man-made surface features such as rail track, roads, canals etc. from the final lineament map.

## Preparation of thematic layers

We utilized eight conditioning parameters such as geology, lineament, slope, drainage density, rainfall, soil texture and depth, and well density to prepare groundwater potential maps. Lithology maps were digitized from the geological quadrangle map, acquired from the Geological Survey of India (GSI). The slope maps were derived directly from SRTM DEM using surface tools in ArcGIS. The stream network vectors were used to prepare the drainage density map using line density tool. Same approach was taken to prepare lineament density raster.

**Table 1** Morphometric parameters and corresponding formulae

| Sr. no. | Parameters                      | Formulae  | References               |
|---------|---------------------------------|---|--------------------------|
| 1       | Stream order (u)                | Hierarchical rank   | Strahler (1964)          |
| 2       | Stream number (Nu)              | Number of streams in each order   | Horton (1945)            |
| 3       | Stream length (Lu)              | Length of stream  | Horton (1945)            |
| 4       | Mean stream length ( $L_{sm}$ ) | $L_{sm} = Lu/Nu$  | Strahler (1964)          |
| 5       | Bifurcation ratio (Rb)          | $Rb = Nu/(Nu + 1)$  | Schumm (1956)            |
| 6       | Mean bifurcation ratio (Rbm)    | Rbm = Average bifurcation ratio of all order  | Strahler (1957)          |
| 7       | Drainage density (Dd)           | $Dd = Lu/A$   | Horton (1945)            |
| 8       | Stream frequency (Sf)           | $Sf = Nu/A$   | Horton (1945)            |
| 9       | Drainage texture (T)            | $T = Dd \times Sf$  | Smith (1950)             |
| 10      | Circularity ratio (Rc)          | $Rc = 4\pi A/P^2$   | Strahler (1964)          |
| 11      | Elongation ratio (Re)           | $Re = D/L = 1.128 \sqrt{A}/L$   | Schumm (1956)            |
| 12      | Form factor (Ff)                | $Ff = A/L^2$  | Horton (1945)            |
| 13      | Relief (R)                      | $R = H - h$   | Hadley and Schumm (1961) |
| 14      | Relief ratio (Rh)               | $Rh = R/L$  | Schumm (1963)            |
| 15      | Hypsometric integral (Hi)       | $Hi = (\text{mean elevation} - \text{min elevation})/(\text{max elevation} - \text{min elevation})$ | Pike and Wilson (1971)   |

We obtained grid based daily rainfall data (1950–2013) from India Meteorological Department (IMD). Mean rainfall and rainfall intensity for each pixel were calculated and maps were constructed. The average annual rainfall was divided by 365 days to obtain rainfall intensity. We acquired soil texture and depth data from National Bureau of Soil Survey and Land Use Planning (NBSS-LUP) regional office in Nagpur. These datasets were digitized in ArcGIS to prepare soil texture and soil depth map. Topographical maps of 1:50,000 scale were used to digitize all the wells available in the study area. 70% of the wells available in each basin were selected randomly for training the FR model and rest 30% wells were used to validate both FR and IF models. Using this well inventory (the training data) the well density maps was produced.

## Determination of groundwater potential zones

### Frequency ratio

Frequency ratio is the prospect of occurrence of a certain factor (Bonham-Carter 1994). The frequency ratio is build upon the relationship between observational well availability and the factors influence the groundwater potential. Frequency ratio of each parameter can be calculated using the following formula:

$$FR = \left[ \frac{P_{gw}/T_{gw}}{P_f/T_f} \right], \quad (1)$$

where FR is frequency ratio,  $P_{gw}$  is the number of pixels with wells in each sub-category,  $T_{gw}$  is the total number of

wells,  $P_f$  is the number of pixels in the classes of a sub-category,  $T_f$  is the total number of pixels in each factor (sum of all sub-category of a certain factor).

Table 2 depicts the frequency ratio for each factor considered in this study to prepare the groundwater potential maps. According to FR calculation, values were assigned to all factors. Later, all the parameters were integrated in ArcGIS and the groundwater potential maps were calculated using the following expression:

$$GPZ = \sum_{i=1}^n FR, \quad (2)$$

Equation (2) can be re-written in simplified form as

$$GPZ = LG_{FR} + SL_{FR} + DD_{FR} + LD_{FR} + RI_{FR} + ST_{FR} + SD_{FR} + WD_{FR}, \quad (3)$$

where LG is lithology, SL is slope, DD is drainage density, LD is lineament density, RI is rainfall intensity, ST is soil texture, SD is soil depth, WD is well density, and FR is the frequency ratio value.

### Influence factor technique

Influence factor technique is a simple overlay based model where weights and ranks are assigned based on the researcher's knowledge on different parameters and their influence in groundwater potential (Das 2019a; Doke 2019). The ranks and weights were assigned to each parameter and their sub-categories based on previous literature review (see Table 3 for weights; and Table 4 for literatures). Consequently, the maps were constructed using the following expression in the ArcGIS environment:

**Table 2** Rank and weight assessment using FR and IF technique for Savitri basin

| Parameters        | Sub-class   | Frequency ratio (FR) |          |       |         |      | Influencing factor(IF) |                |
|-------------------|-------------|----------------------|----------|-------|---------|------|------------------------|----------------|
|                   |             | Pixels count         | % Pixels | Wells | % wells | FR   | Weight ( $W_i$ )       | Rank ( $R_i$ ) |
| Geology           | Basalt      | 261,897              | 0.94     | 461   | 0.93    | 1.00 | 20                     | 10             |
|                   | Laterite    | 17,416               | 0.06     | 33    | 0.07    | 1.07 |                        | 20             |
| Slope             | 0–5.27      | 104,663              | 0.37     | 311   | 0.63    | 1.68 | 16                     | 16             |
|                   | 5.27–12.30  | 73,697               | 0.26     | 139   | 0.28    | 1.07 |                        | 13             |
|                   | 12.30–20.08 | 58,371               | 0.21     | 40    | 0.08    | 0.39 |                        | 10             |
|                   | 20.08–31.38 | 31,993               | 0.11     | 4     | 0.01    | 0.07 |                        | 7              |
|                   | 31.38–64.02 | 10,589               | 0.04     | 0     | 0.00    | 0.00 |                        | 4              |
| Drainage density  | 0–0.57      | 28,223               | 0.10     | 32    | 0.06    | 0.64 | 15                     | 3              |
|                   | 0.57–0.82   | 67,561               | 0.24     | 95    | 0.19    | 0.80 |                        | 6              |
|                   | 0.82–1.04   | 78,104               | 0.28     | 127   | 0.26    | 0.92 |                        | 9              |
|                   | 1.04–1.28   | 70,354               | 0.25     | 153   | 0.31    | 1.23 |                        | 12             |
|                   | 1.28–1.84   | 35,071               | 0.13     | 87    | 0.18    | 1.40 |                        | 15             |
| Lineament density | 0–0.07      | 110,332              | 0.40     | 224   | 0.45    | 1.15 | 13                     | 5              |
|                   | 0.07–0.21   | 67,217               | 0.24     | 112   | 0.23    | 0.94 |                        | 7              |
|                   | 0.21–0.37   | 48,514               | 0.17     | 87    | 0.18    | 1.01 |                        | 9              |
|                   | 0.37–0.57   | 37,801               | 0.14     | 61    | 0.12    | 0.91 |                        | 11             |
|                   | 0.57–1.02   | 15,449               | 0.06     | 10    | 0.02    | 0.37 |                        | 13             |
| Rainfall          | 8.59–9.74   | 119,272              | 0.43     | 218   | 0.44    | 1.03 | 10                     | 2              |
|                   | 9.74–10.57  | 62,390               | 0.22     | 132   | 0.27    | 1.20 |                        | 4              |
|                   | 10.57–11.52 | 48,740               | 0.17     | 76    | 0.15    | 0.88 |                        | 6              |
|                   | 11.52–12.65 | 30,169               | 0.11     | 42    | 0.09    | 0.79 |                        | 8              |
|                   | 12.65–14.45 | 18,742               | 0.07     | 26    | 0.05    | 0.78 |                        | 10             |
| Soil texture      | Sand        | 7861                 | 0.03     | 28    | 0.06    | 2.01 | 9                      | 5              |
|                   | Loam        | 196,973              | 0.71     | 326   | 0.66    | 0.94 |                        | 9              |
|                   | Clay        | 74,479               | 0.27     | 140   | 0.28    | 1.06 |                        | 7              |
| Soil depth        | Shallow     | 191,199              | 0.68     | 317   | 0.64    | 0.94 | 9                      | 5              |
|                   | Mod deep    | 80,253               | 0.29     | 154   | 0.31    | 1.08 |                        | 7              |
|                   | Deep        | 7861                 | 0.03     | 23    | 0.05    | 1.65 |                        | 9              |
| Well density      | 0–0.14      | 106,136              | 0.38     | 61    | 0.12    | 0.32 | 8                      | 2              |
|                   | 0.14–0.30   | 92,571               | 0.33     | 182   | 0.37    | 1.11 |                        | 3              |
|                   | 0.30–0.45   | 54,656               | 0.20     | 146   | 0.30    | 1.51 |                        | 4              |
|                   | 0.45–0.71   | 21,514               | 0.08     | 75    | 0.15    | 1.97 |                        | 6              |
|                   | 0.71–1.11   | 4436                 | 0.02     | 30    | 0.06    | 3.82 |                        | 8              |

$$GPZ = \sum_{i=0}^n (W_i \times R_i), \tag{4}$$

where  $W_i$  is the weight of each factor,  $R_i$  is the rank of each sub-category.

## Results and discussion

The results of this study are categorized into two major parts. The first section describes the morphometric analysis through drainage quantification and terrain measurement in the study area. The second section will give a

comprehensive description of different influencing parameters and the groundwater potentiality of the study area. The significant results are discussed below.

### Morphometric analysis

#### Stream order ( $u$ )

Strahler (1964) proposed that streams in a basin can be categorized on the hierarchical basis. At the upstream, first order is the streams having no tributaries; second order starts when two first-order streams join and the count goes on. Savitri and Vashisthi basins are classified as sixth-order drainage basins. There is a significant negative

**Table 3** Rank and weight assessment using FR and IF technique for Vashisthi basin

| Parameters        | Sub-class   | Frequency ratio (FR) |          |       |         |      | Influencing factor(IF) |                |
|-------------------|-------------|----------------------|----------|-------|---------|------|------------------------|----------------|
|                   |             | Pixels count         | % Pixels | Wells | % wells | FR   | Weight ( $W_i$ )       | Rank ( $R_i$ ) |
| Geology           | Basalt      | 230,020              | 0.86     | 633   | 0.83    | 0.96 | 20                     | 10             |
|                   | Laterite    | 37,135               | 0.14     | 130   | 0.17    | 1.23 |                        | 20             |
| Slope             | 0–5.36      | 90,701               | 0.34     | 475   | 0.62    | 1.83 | 16                     | 16             |
|                   | 5.36–11.71  | 80,598               | 0.30     | 233   | 0.31    | 1.01 |                        | 13             |
|                   | 11.71–19.03 | 53,761               | 0.20     | 42    | 0.06    | 0.27 |                        | 10             |
|                   | 19.03–29.53 | 32,727               | 0.12     | 12    | 0.02    | 0.13 |                        | 7              |
|                   | 29.53–62.23 | 9368                 | 0.04     | 1     | 0.00    | 0.04 |                        | 4              |
| Drainage density  | 0–0.54      | 17,405               | 0.07     | 66    | 0.09    | 1.33 | 15                     | 3              |
|                   | 0.54–0.77   | 45,697               | 0.17     | 82    | 0.11    | 0.63 |                        | 6              |
|                   | 0.77–0.95   | 76,596               | 0.29     | 182   | 0.24    | 0.83 |                        | 9              |
|                   | 0.95–1.14   | 80,983               | 0.30     | 257   | 0.34    | 1.11 |                        | 12             |
|                   | 1.14–1.61   | 46,474               | 0.17     | 176   | 0.23    | 1.33 |                        | 15             |
| Lineament density | 0–0.12      | 83,418               | 0.31     | 305   | 0.40    | 1.28 | 13                     | 5              |
|                   | 0.12–0.29   | 91,605               | 0.34     | 257   | 0.34    | 0.98 |                        | 7              |
|                   | 0.29–0.47   | 54,408               | 0.20     | 131   | 0.17    | 0.84 |                        | 9              |
|                   | 0.47–0.75   | 27,564               | 0.10     | 60    | 0.08    | 0.76 |                        | 11             |
|                   | 0.75–1.40   | 10,160               | 0.04     | 10    | 0.01    | 0.34 |                        | 13             |
| Rainfall          | 7.38–8.23   | 41,530               | 0.16     | 146   | 0.19    | 1.23 | 10                     | 2              |
|                   | 8.23–8.73   | 68,288               | 0.26     | 257   | 0.34    | 1.32 |                        | 4              |
|                   | 8.73–9.27   | 61,097               | 0.23     | 215   | 0.28    | 1.23 |                        | 6              |
|                   | 9.27–9.83   | 55,112               | 0.21     | 104   | 0.14    | 0.66 |                        | 8              |
|                   | 9.83–10.74  | 41,128               | 0.15     | 41    | 0.05    | 0.35 |                        | 10             |
| Soil texture      | Sand        | 5541                 | 0.02     | 18    | 0.02    | 1.14 | 9                      | 5              |
|                   | Loam        | 229,819              | 0.86     | 695   | 0.91    | 1.06 |                        | 9              |
|                   | Clay        | 31,795               | 0.12     | 50    | 0.07    | 0.55 |                        | 7              |
| Soil depth        | Shallow     | 121,070              | 0.45     | 276   | 0.36    | 0.80 | 9                      | 5              |
|                   | Mod deep    | 139,699              | 0.52     | 466   | 0.61    | 1.17 |                        | 7              |
|                   | Deep        | 6386                 | 0.02     | 21    | 0.03    | 1.15 |                        | 9              |
| Well density      | 0–0.14      | 68,768               | 0.26     | 18    | 0.02    | 0.09 | 8                      | 2              |
|                   | 0.14–0.35   | 89,429               | 0.33     | 187   | 0.25    | 0.73 |                        | 3              |
|                   | 0.35–0.65   | 68,872               | 0.26     | 267   | 0.35    | 1.36 |                        | 4              |
|                   | 0.65–0.96   | 31,998               | 0.12     | 203   | 0.27    | 2.22 |                        | 6              |
|                   | 0.96–1.52   | 8088                 | 0.03     | 88    | 0.12    | 3.81 |                        | 8              |

correlation can be found between the stream order and stream number (Fig. 2). In all the natural river systems, as the stream order increases, stream number decreases.

### Mean stream length ( $L_{sm}$ )

Mean stream length ( $L_{sm}$ ) epitomizes the characteristic size of the components of a drainage network and its contributing basin surface area.  $L_{sm}$  can be computed by dividing total the length of streams in an order to the sum of all the streams of the same order. Table 5 represents the variation of  $L_{sm}$  for Savitri and Vashisthi basins (0.78–54.23 and 0.84–52.14). According to Horton's (1945) law,  $L_{sm}$  against the stream

order in a semi-logarithmic scale makes a straight trend line. This relation indicates the erosion laws which are acting on the geological material along with similar weathering-erosion characteristics of the drainage basin evolution. Anomalies in this relationship could be followed by structural control over an area.

### Bifurcation ratio ( $R_b$ )

The degree of structural and lithological control over an area can be determined using bifurcation ratio. This parameter is a fundamental study to understand the tectonic or structural anomalies of a drainage network.

**Table 4** Table of the parameters that were used in different studies for groundwater potential zonation

| Paper name                          | S | GL | Dd | G | LD | E | So | LU | NDVI | Geom | R | TWI |
|-------------------------------------|---|----|----|---|----|---|----|----|------|------|---|-----|
| Mokadem et al. (2018)               | * |    | *  | * |    |   |    |    |      |      |   |     |
| Nsiah et al. (2018)                 |   |    |    |   |    |   |    |    |      |      |   |     |
| Nigussie et al. (2019)              | * |    | *  | * | *  | * | *  | *  |      | *    | * |     |
| Yousef et al. (2015)                | * |    | *  | * | *  |   |    |    |      | *    |   |     |
| Venkateswaran and Ayyandurai (2015) | * |    | *  | * | *  |   |    |    |      | *    |   |     |
| Kumar and Pandey (2016)             | * | *  | *  | * | *  |   |    |    |      | *    |   |     |
| Rizeei et al. (2019)                | * |    |    | * |    | * |    | *  |      |      |   | *   |
| Chen et al. (2018)                  | * |    |    | * |    | * | *  | *  | *    |      |   | *   |
| Arabameri et al. (2019)             | * | *  | *  | * |    | * | *  | *  |      |      | * | *   |
| Ganapuram et al. (2009)             | * |    | *  | * | *  |   |    | *  |      | *    |   |     |
| Adeyeye et al. (2019)               | * |    | *  | * | *  | * | *  |    |      |      |   |     |
| Yeh et al. (2016)                   | * |    | *  | * | *  |   |    | *  |      |      |   |     |
| Abijith et al. (2020)               | * |    | *  | * | *  |   | *  | *  |      | *    | * |     |
| Pham et al. (2019)                  | * |    | *  | * |    | * | *  | *  |      |      | * | *   |
| Patra et al. (2018)                 | * |    |    | * |    | * | *  | *  | *    | *    | * |     |
| Pal et al. (2020)                   | * | *  |    | * |    | * | *  | *  | *    |      | * | *   |
| Balamurugan et al. (2017)           | * | *  | *  |   | *  |   |    | *  |      | *    |   |     |
| Misi et al. (2018)                  | * |    | *  | * |    | * |    | *  |      |      | * | *   |
| Magesh et al. (2012)                | * |    | *  | * | *  |   | *  | *  |      |      | * |     |
| Andualem and Demeke (2019)          | * |    | *  | * | *  |   | *  | *  |      | *    |   |     |
| Berhanu and Hatiye (2020)           | * |    | *  | * | *  | * | *  | *  |      | *    | * |     |
| Nithya et al. (2019)                | * |    | *  | * | *  |   | *  | *  |      | *    | * |     |
| Etikala et al. (2019)               | * |    | *  | * | *  |   | *  | *  |      | *    | * |     |
| Raju et al. (2019)                  | * |    | *  | * | *  | * | *  | *  |      | *    | * |     |
| Ahmed and Sajjad (2018)             | * | *  | *  | * | *  | * | *  | *  |      |      | * |     |
| Kumar et al. (2020)                 | * |    | *  | * | *  |   | *  | *  |      | *    |   |     |
| Gnanachandrasamy et al. (2018)      | * |    | *  | * | *  |   | *  |    |      | *    | * |     |
| Kanagaraj et al. (2019)             | * |    | *  | * | *  |   | *  | *  |      | *    | * |     |
| Mahato and Pal (2019)               | * | *  |    | * | *  | * | *  | *  | *    |      | * |     |
| Pande et al. (2019)                 | * |    | *  |   |    | * |    | *  |      | *    |   |     |
| Preeja et al. (2011)                | * |    | *  | * | *  |   | *  | *  |      | *    |   |     |
| Rao (2006)                          | * | *  | *  |   | *  |   | *  | *  |      | *    | * |     |
| Thapa et al. (2017)                 | * |    | *  | * | *  | * | *  | *  |      | *    | * |     |
| Das et al. (2017)                   | * |    | *  | * | *  |   | *  | *  |      | *    | * |     |
| Das and Pardeshi (2018b)            | * |    | *  | * | *  |   | *  | *  |      | *    | * |     |
| Das (2019b)                         | * | *  | *  | * | *  |   | *  | *  |      | *    | * |     |

S slope, GL groundwater level, Dd drainage density, G geology, LD lineament density, E elevation, So soil, LU landuse, NDVI normalized differential vegetation index, Geom geomorphology, R rainfall, TWI topographic wetness index

Schumm (1956) demonstrated bifurcation ratio as the ratio of the number of streams in an order to the number of streams in the higher order in the catchment. In ordinary cases, the bifurcation ratio varies between 3 and 5, except places where strong geological control predominates (Das 2018a). Mean bifurcation ratio of Savitri and Vashisthi basins are 4.35 and 4.25, respectively. Very low mean bifurcation ratio of these basins is indicating geological structures do not have significant dominance on the drainage network (Chow 1964; Sreedevi et al. 2009; Pandey and

Das 2016). A strong relationship between drainage pattern and bifurcation ratio can be found. Regions having parallel or rectangular drainage pattern show higher bifurcation ratio compared to dendritic or trellised drainage pattern.

#### Drainage density ( $D_d$ )

Horton (1932) demonstrated drainage density as the ratio between the total length of streams within a basin and the

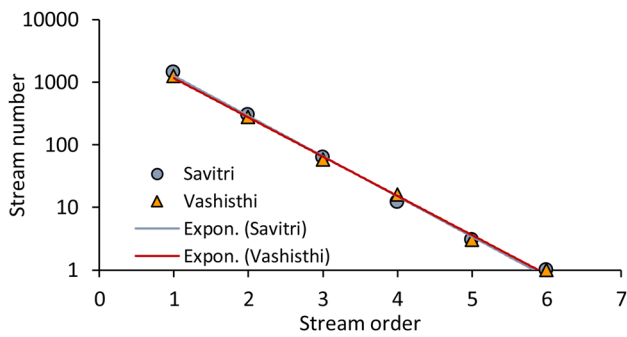


**Fig. 2** Relationship between stream order and stream number. As the stream order increases in a drainage basin, number of streams decreases significantly

basin area. Drainage density represents the closeness of spacing of streams. Factors such as geology, slope, and relief control the drainage density of an area significantly. Region having lower relief shows lower drainage density compared to the higher relief area (Strahler 1964). Drainage density of Savitri and Vashisthi basins are 0.97 and 0.93 km/km<sup>2</sup>, respectively. Lower drainage density on both basins represents homogeneous lithology, slope, and relief characteristics.

**Stream frequency ( $S_f$ )**

According to Horton (1932), stream frequency can be defined as total number of streams per unit area. Stream frequency values for Savitri and Vashisthi are 0.80 and 0.74, respectively, (Table 5). Stream frequency of a drainage basin mainly depends on the lithology and structural character of a drainage basin.

**Drainage texture ( $T$ )**

Smith (1950) demonstrated that lithology, climate, catchment relief, infiltration capacity, vegetation cover, and the stage of drainage development are the prime factors to regulate the drainage texture. Coarse drainage texture can be found where lithology is characterized by massive hard rock. Conversely, a region having soft or wear rock shows fine drainage texture. Drainage texture of a basin is merely the product of drainage density and stream frequency. Very coarse drainage texture is exhibited by Savitri and Vashisthi mainly because of the hard rock basaltic terrain.

**Circularity ratio ( $R_c$ )**

Strahler (1964) introduced circularity ratio as the ratio of the basin area to the area of a circle having same perimeter of the drainage basin.  $R_c$  values of 1 indicate circular basin shape and similar infiltration capacity over the entire basin. Lower values of  $R_c$  represents lower infiltration rate is very low and occurrence of high-velocity runoff can be observed.  $R_c$  values of Savitri and Vashisthi basin are 0.28 and 0.34. Moderate values of  $R_c$  indicate both basins are characterized by mature stage of drainage development.

**Elongation ratio ( $R_e$ )**

Elongation ratio ( $R_e$ ) of a basin is the ratio between the diameter of a circle having the same area as the basin and total length of the basin (Schumm 1956).  $R_e$  of a drainage basin indicates the shape of the basin where  $R_e$  value of 1 indicates perfect circular basin. For elongated basins,  $R_e$  value becomes close to 0. Table 6 shows the classification

**Table 5** Results of drainage network properties in Vaitarna and Ulhas basins

| Basin name | Stream order (u) | Stream number (Nu) | Stream length (Lu) (Km) | Mean stream length (Lsm) (km) | Bifurcation ratio (Rb) | Mean bifurcation ratio (Rbm) |
|------------|------------------|--------------------|-------------------------|-------------------------------|------------------------|------------------------------|
| Savitri    | I                | 1429               | 1114.99                 | 0.78                          | –                      | 4.35                         |
|            | II               | 296                | 555.74                  | 1.88                          | 4.83                   |                              |
|            | III              | 62                 | 259.09                  | 4.18                          | 4.77                   |                              |
|            | IV               | 12                 | 135.50                  | 11.29                         | 5.17                   |                              |
|            | V                | 3                  | 65.51                   | 21.84                         | 4                      |                              |
|            | VI               | 1                  | 54.23                   | 54.23                         | 54.23                  | 3                            |
| Vashisthi  | I                | 1248               | 1049.64                 | 0.84                          | –                      | 4.25                         |
|            | II               | 275                | 460.76                  | 1.68                          | 4.54                   |                              |
|            | III              | 58                 | 264.35                  | 4.56                          | 4.74                   |                              |
|            | IV               | 16                 | 168.147                 | 10.51                         | 3.63                   |                              |
|            | V                | 3                  | 15.02                   | 5.01                          | 5.33                   |                              |
|            | VI               | 1                  | 52.14                   | 52.14                         | 52.14                  | 3                            |



of required  $R_e$  values for different shape of basins. Savitri and Vashisthi basins are showing high elongation ratio. It is indicating both of these basins are having moderately circular shape.

### Form factor ( $F_f$ )

In quantitative drainage morphometry, form factor is the dimensionless ratio between basin area and the square of basin length (Horton 1945). There is a direct relationship can be found between form factor to the stream flow and shape of the basin. Lower form factor indicates elongated nature of drainage basin, whereas a higher value indicates rectangular or elongation shape. Form factor values for Savitri and Vashisthi basins are 0.46 and 0.56, respectively, clearly indicate that these basins are having semi-circular shape.

### Relief ( $R$ )

Geomorphic surface processes such as erosional mechanism and mass-movement intensity of an area exclusively depend on the relief of the drainage basin. Basin relief is basically the dissimilarity between the maximum and the minimum elevation within the catchment area. Very high relief basins are generally governed by steep gradients with dominating hillslope processes and slope failures (Das 2020). Comparatively, low-lying flat regions with deep chemical weathering character is the main geomorphic processes in low relief catchments. Also, the materials eroded from high relief zones by fluvial processes generally tend

to deposit on the low relief sections as the stream power becomes lower. Relief of Savitri and Vashisthi basins is 1393 and 1193 m, respectively. Very high relief of Savitri and Vashisthi indicates governing hillslope mechanisms with high-velocity runoff and less infiltration potential of the study area.

### Relief ratio ( $R_h$ )

According to Schumm (1956), relief ratio is a dimensionless metric that is the height–length ratio of horizontal distance to the longest extent of the basin to the principle drainage line. This factor indicates overall steepness and the erosional physiognomies of the drainage basin. Savitri (19.82) and Vashisthi (19.11) basins show very high relief ratio. High relief ratio of these basins indicates very steep slope and higher erosional vulnerability.

### Hypsometric integral ( $H_i$ )

Hypsometric integral of a watershed can be used to determine the geological stage of drainage development (Wood and Snell 1960; Pike and Wilson 1971). Hypsometric integral of a region is the relative proportion of the highland and lowland areas. Savitri and Vashisthi basins show very low hypsometric integral (Table 6). Considering to the Devis's cycle of erosion, both of these basins are falling to the old stage of drainage development.

## Influence of different parameters for groundwater potential

### Lithology

The groundwater potential of a region change place to place depending on lithological variation. Regions having massive plutonic rocks such as granite and diorite generally have very low groundwater potential due to lack of pores. However, volcanic rocks such as basalts can sometimes have pores because of pyroclastic material such as ashes, angular element structures, and vesicular textures. Therefore, basalts are generally having low to medium groundwater potential. Very high groundwater potentials can be found in regions lying on sedimentary rocks such as partially lithified shells, well-sorted fine-grained sandstone, etc. Regions over deep unconsolidated alluvium are having very high groundwater potential as well.

In Savitri and Vashisthi basins, the major rock type is flood basalt, erupted during Cretaceous–Tertiary boundary in the geological time scale about 65 million years ago. Near the coastal regions, some patches of lateritic soil can be observed (Figs. 3 and 4).

**Table 6** Results showing variation of basin morphometric properties of Vaitarna and Ulhas basins

| Sr. no. | Parameters  | Basin name |           |
|---------|---|------------|-----------|
|         |   | Savitri    | Vashisthi |
| 1       | Basin area ( $A$ ) ( $\text{km}^2$ )                  | 2262       | 2163      |
| 2       | Basin perimeter (km)                                  | 315.19     | 280.45    |
| 3       | Basin length ( $L$ ) (km)                             | 70.29      | 62.43     |
| 4       | Basin width ( $W$ ) (km)                              | 65         | 51.38     |
| 5       | Drainage density ( $Dd$ ) ( $\text{km}/\text{km}^2$ ) | 0.97       | 0.93      |
| 6       | Stream frequency ( $Sf$ ) ( $\text{No}/\text{km}^2$ ) | 0.80       | 0.74      |
| 7       | Drainage texture ( $T$ )                              | 0.77       | 0.69      |
| 8       | Circularity ratio ( $R_c$ )                           | 0.28       | 0.34      |
| 9       | Elongation ratio ( $R_e$ )                            | 0.76       | 0.82      |
| 10      | Form factor ( $F_f$ )                                 | 0.46       | 0.56      |
| 11      | Shape factor ( $F_s$ )                                | 2092.01    | 1780.96   |
| 12      | Relief ( $R$ )  | 1393       | 1193      |
| 13      | Relief ratio ( $R_h$ )                                | 19.82      | 19.11     |
| 14      | Hypsometric integral ( $H_i$ )                        | 0.14       | 0.17      |

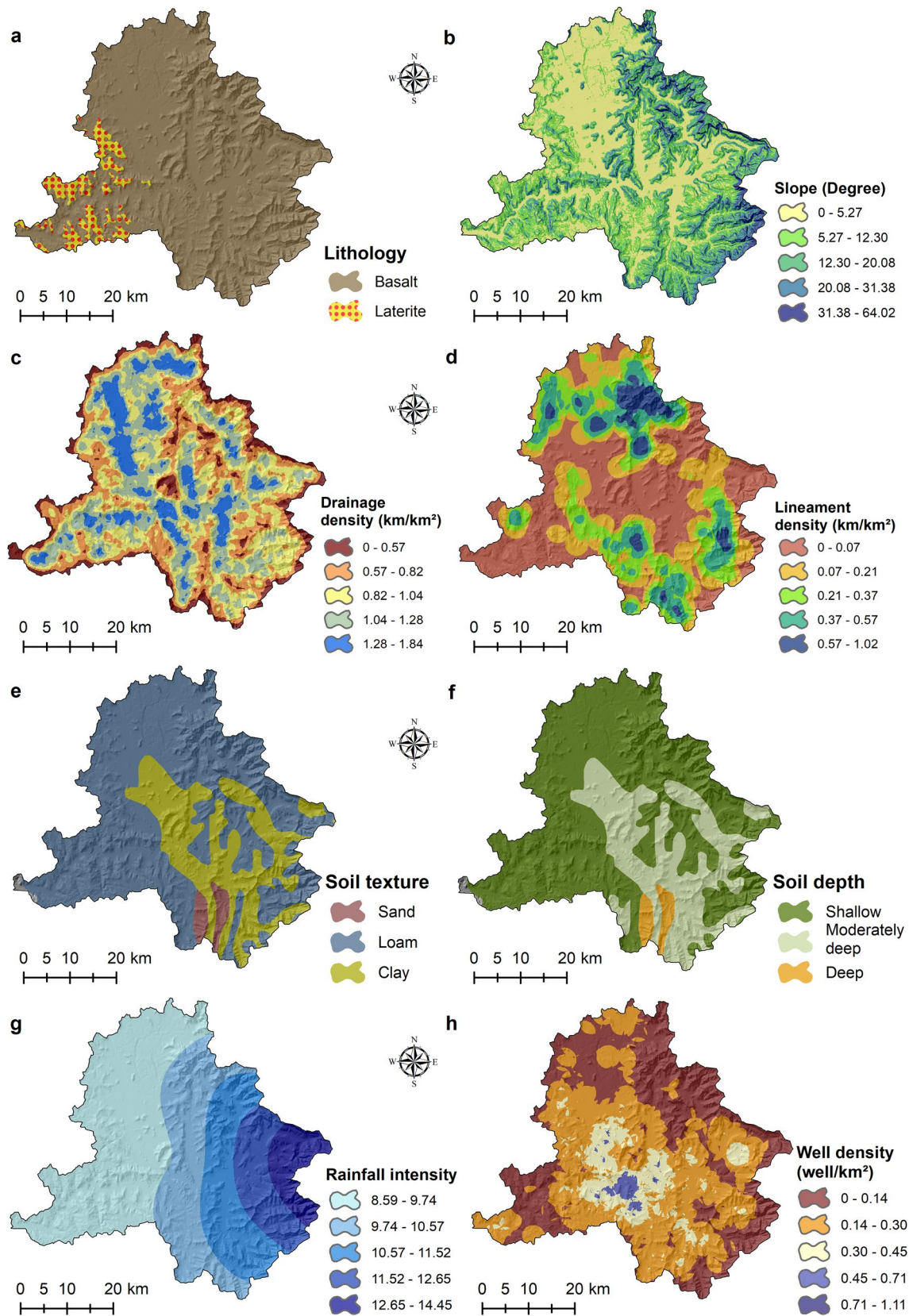


**Fig. 3** Geo-environmental parameters considered in this study to map different groundwater potential zones in Savitri basin. **a** Lithology, **b** slope, **c** drainage density, **d** lineament density, **e** soil texture, **f** soil depth, **g** rainfall, **h** well density

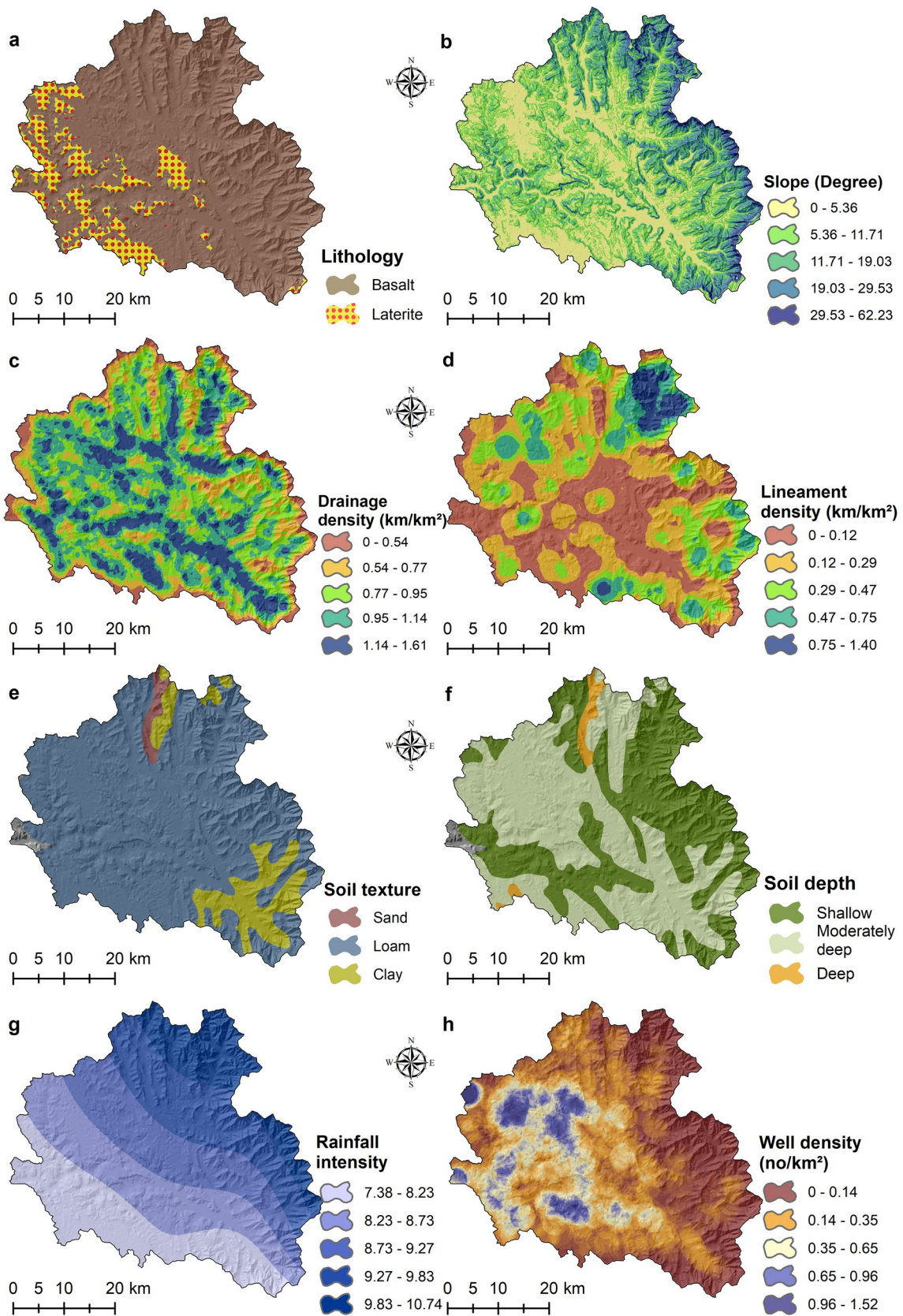


**Fig. 4** Geo-environmental parameters considered in this study to map different groundwater potential zones in Vashisthi basin. **a** Lithology, **b** slope, **c** drainage density, **d** lineament density, **e** soil texture, **f** soil depth, **g** rainfall, **h** well density

## Slope

Slope is the degree of inclination of a region concerning to the horizontal surface. Understanding the slope of a region is necessary for many purposes such as agriculture, planning, construction of engineering structures, groundwater potential assessment, flood mapping, landslides etc. (Pham et al. 2020). The slope of a region is controlled by variation in lithology with different rate of resistance, different geomorphic processes, and climate. Regions having a very low slope are generally having higher groundwater potential. The slope variation in Savitri and Vashisthi basins are ranging from  $0^\circ$  to  $64^\circ$  and  $0^\circ$  to  $62^\circ$ , respectively, (Figs. 3 and 4).

## Drainage density

Earlier, many researchers described that region having a lower drainage density is generally having higher groundwater potentiality due to the impermeable lithology (Bagyaraj et al. 2013; Jenifer and Jha 2017; Thomas and Duraisamy 2017). However, it is evident that irrespective of lithological variation, water generally follow the slope and accumulate on the lower surface elevation of an area. Therefore, when lithology is considered, if the streams are flowing through the porous rocky surface, there will be a substantial amount of recharge from the stream itself, if the groundwater level is lower than the river bed. This phenomenon is more evident and effective in arid and semi-arid regions, where groundwater levels during most of the season stays below the river bed.

## Lineament density

Lineaments are the linear or curvy linear feature on the earth's surface which can be seen and mapped using satellite images (Marghany 2012). There is a significant importance of availability of lineaments with the groundwater potential of an area. Lineaments are weaknesses in the rock, play a crucial role in the infiltration process in the hard rock region (Das et al. 2018). Savitri and Vashisthi basins show numerous lineaments which are generally mafic basaltic dykes with an orientation in NNE–SSW and N–S direction (Figs. 3 and 4) (Das and Pardeshi 2018b).

## Rainfall intensity

Occurrence of rainfall can be observed anywhere on the earth except the polar regions (Das 2018b). However, in some region, the intensity is very high while some places characterize very low intensity rainfall. Savitri and Vashisthi

basins show a semi-arid climatic condition where rainfall occurs during monsoon months. In this region, rainfall is the only source of groundwater. Rainfall intensity is very high in the escarpment section and decreases gradually in the coastal region (Figs. 3 and 4).

## Soil texture

There is a direct relationship between groundwater potential and soil texture of a region can be found. Soils which are moderately cohesive such as sandy loam and loam generally have higher groundwater potential. By contrast, soils which are highly compacted such as clay and silt generally have low groundwater potential due to the insufficient availability of soil pores.

## Soil depth

Regions having very deep soil generally have higher groundwater potentiality as the water can infiltrate to the depth. Conversely, regions having shallow soil have lower potentiality of groundwater due to the massive bed rock, which partially works as an aquifuge layer, beneath the soil which prevent the water to infiltrate.

## Well density

Before the technological advancement, the wells used to be built based on the availability of water in nearby wells which were built previously. Therefore, it can be observed that more number of wells are located only in the regions having higher yield of groundwater. Therefore, by including well density of a region, the extraction of different groundwater potential zones can be more accurate.

## Groundwater potential analysis

The frequency ratio model is based on the relationship between the occurrence and their contributing area. The maps as a result of frequency ratio is being categorized into four groundwater potential zones—very high, high, moderate, and low (Fig. 5). Using this model, Savitri and Vashisthi basin show 9% and 17% of the total area are having very high, 30% and 32% are having high, 38% and 26% are having moderate, 23% and 25% are having low groundwater potential, respectively, (Fig. 6). The overall analysis shows that Vashisthi is contributing more areas with high groundwater potential compared to the Savitri basin.

While the maps are prepared through influencing factor technique for Savitri and Vashisthi basin, they show that

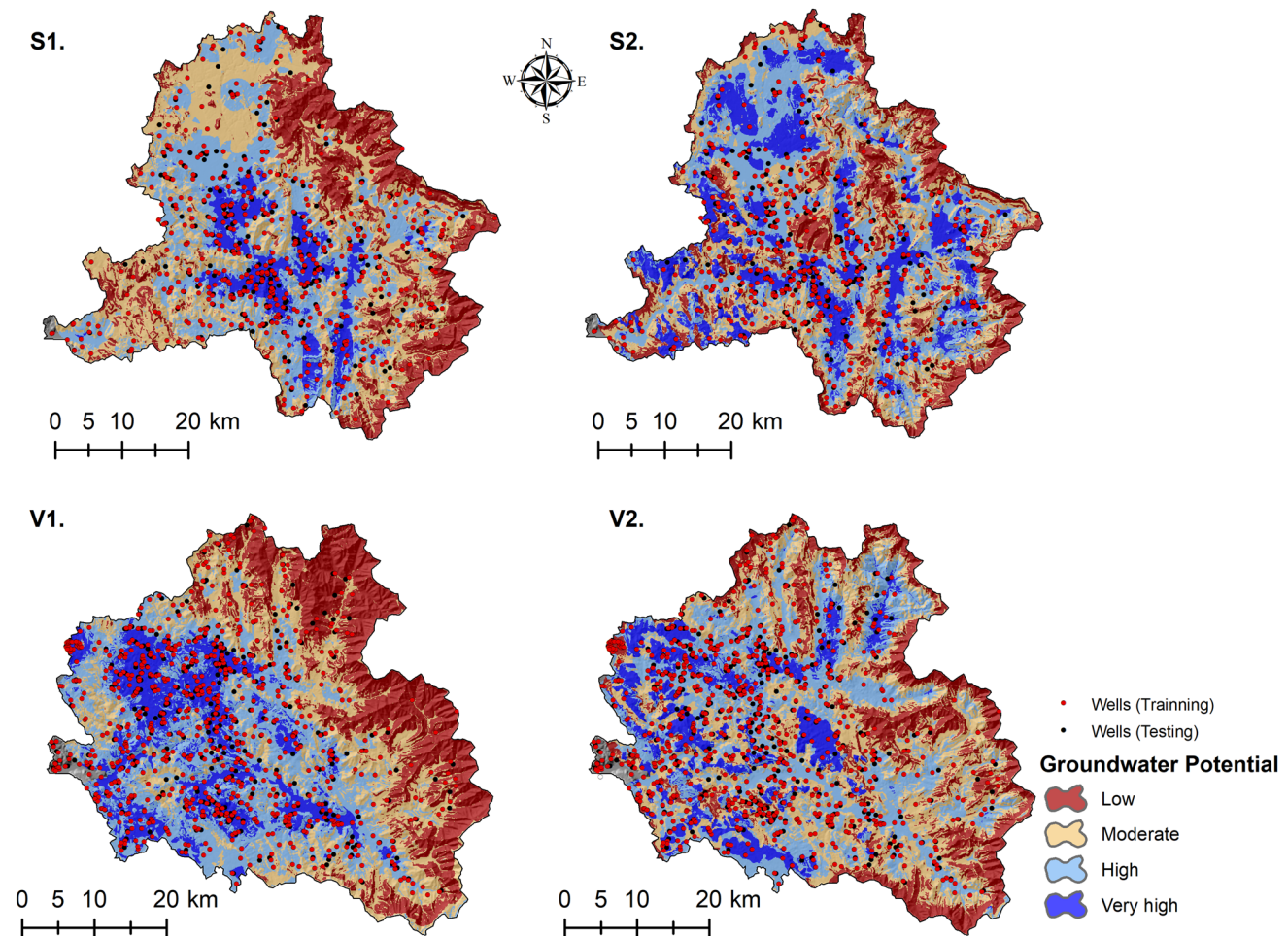


**Fig. 5** The groundwater potential map of Savitri and Vashisthi basins. Notice the inset red and black dots which are well inventories used for training and testing the FR models. S1. Savitri (FR), S2. Savitri (IF), V1. Vashisthi (FR), V2. Vashisthi (IF)

about 21% and 13% areas are covering very high, 33 and 34% are having high, 29% and 34% are having moderate, 18% and 19% area are covering low groundwater prospect, respectively, (Fig. 6).

Both catchments show a higher groundwater potential towards low-lying flat downstream section near the coast. The highlands in west and central hilly regions are characterized by very low groundwater potential because of the very steep gradient, the presence of massive basaltic hard rock, low drainage density, and shallow soil depth. Our study makes a notable observation that the regions with high-density lineaments are not entirely having very high groundwater potentials. This is probably because of the other factors such as lithology, soil cover, and gradient. However, these regions may influence the subsurface water recharge.

## Validation

The area under the curve is a simple and convenient technique for validation of multi-criteria-based GIS models (Pradhan and Lee 2010; Bui et al. 2011). Validation of both models is done based on the area under the curve (AUC) method. To run frequency ratio, 70% of the total number of wells is used as training data and 30% is used for testing or validating the models. The same well inventory (30%) is used as a proxy of groundwater yield to validate the IF model. We have divided the output results (groundwater potential scores) into 20 equal classes. Then, we have plotted the cumulative area under different groundwater potential in “X” axis, while the cumulative number of wells in each class has been plotted in “Y” axis. Then, the AUC has been calculated using the following formula:

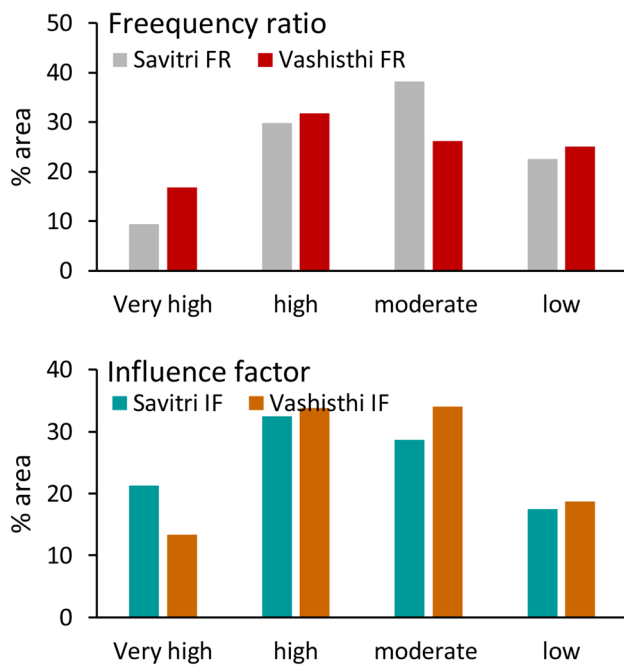


**Fig. 6** Bar graphs are showing the percentage of areas under different groundwater potential classes in Savitri and Vashisthi basins

$$AUC = \sum_{i=1}^{n=20} \frac{(X_1 + X_2)}{2(Y_2 - Y_1)}, \quad (5)$$

where AUC denotes area under the curve,  $X$  indicates the cumulative percentage of different groundwater potential area,  $Y$  indicates cumulative percentage of wells, 1 and 2 designate two sequential points of data and  $n$  is the number of groundwater potential classes.

The AUC curve shows that Savitri and Vashisthi basins are having same efficiency (75%) in case of FR model (Fig. 7). By contrast, the accuracy of the IF model for Savitri and Vashisthi is 69% and 65%. Therefore, it can be clearly understood that the efficiency of FR model is better than IF model. Additionally, the accuracy of the IF model lies on the researcher's knowledge of different parameters and assignment of scores which can lead to inaccurate results (Das 2019a).

Earlier, several studies were carried out to map groundwater potential zones utilizing the frequency ratio model (Manap et al. 2014; Al-Abadi et al. 2016, 2017; Das and Pardeshi 2018c). Almost all these studies indicated found fairly accurate results. Manap et al. (2014) applied frequency ratio to map groundwater potentials in Malaysia and found a high accuracy (85%). Groundwater prediction by Al-Abadi et al. (2016) showed the prediction rate of frequency ratio as high as 80%. The work of Balamurugan et al. (2017), which was applied in semi-arid India, showed a considerable groundwater map accuracy (77%). Das and Pardeshi (2018a,

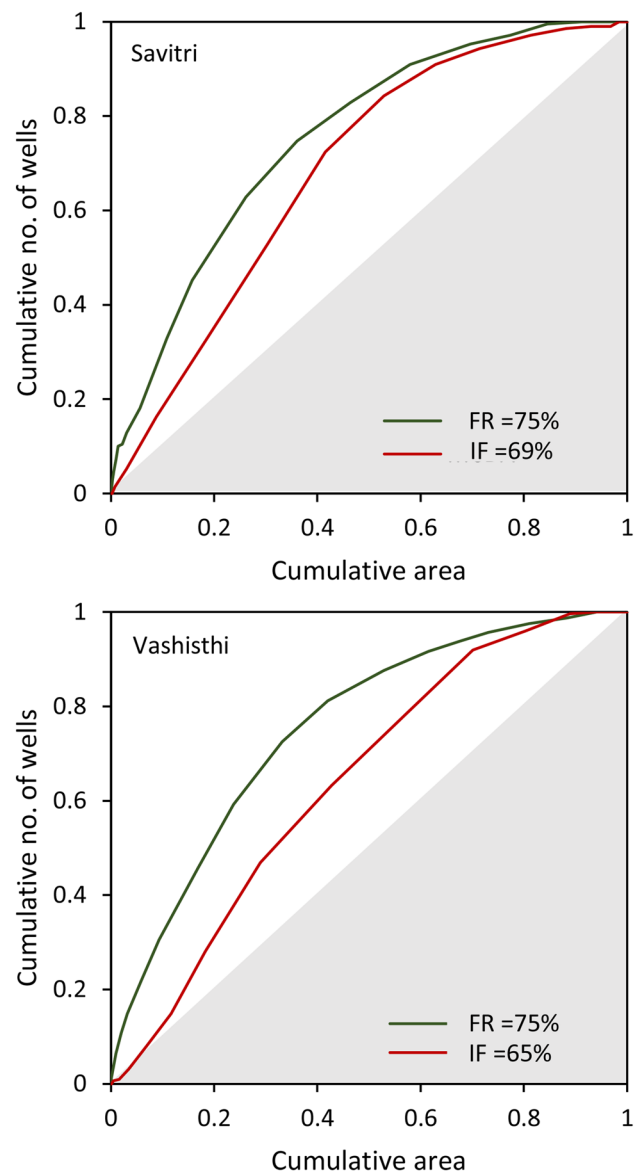


**Fig. 7** Cumulative number of wells available in the study area are plotted against cumulative area under different groundwater potential zones for the assessment of accuracy of FR and IF models. The AUC for FR and IF is calculated for both the basins. The overall accuracy is higher in case of FR compared to IF technique in both basins

b, c) presented a comparison between influencing factor and frequency ratio and demonstrated higher reliability of the model while done through frequency ratio.

Besides AUC, we have compared the output results with published reports of CGWB of Raigarh and Ratnagiri district. It is found that the groundwater yield in the hilly regions is very low (< 0.5 lps), while in the central and coastal region, the yield is very high (3–10 lps). Therefore, this study can be considered as highly accurate for groundwater potential mapping of Savitri and Vashisthi basins.

## Conclusion

The major aim of this study was to perform morphometric analysis and groundwater potential mapping of two semi-arid catchments in Maharashtra, India, utilizing frequency ratio and influencing factor techniques. Eight factors that influence the groundwater potential were assessed in GIS to built groundwater potential maps. The morphometric analyses suggested that Savitri and Vashisthi basins belong to mature or near-old stage of drainage development. The groundwater potential maps derived from the frequency ratio for Savitri and Vashisthi show that 9% and 17% are very high, 30% and 32% are high, 38% and 26% are moderate, 23% and 25% are encompassing low groundwater potential, respectively. On the other hand, the groundwater map predicted using influencing factor technique indicated about 21% and 13% very high, 33 and 34% high, 29% and 34% moderate, 18% and 19% low groundwater prospect for Savitri and Vashisthi basins, respectively. The comparison between FR and IF technique suggested that FR technique is more reliable (AUC = 75% for both basins) than the IF technique (AUC = 69% for Savitri and 65% for Vashisthi). This, among these two techniques, the FR has exceptionally high prediction accuracy for groundwater mapping. The outcomes of the present study might be helpful as fast-hand information to the local governing agencies and administrative bodies for the assessment, management, administration, planning, and sustainable utilization of groundwater and artificial recharge in the near future.

**Acknowledgements** The authors wish to thank NBSS LUP officials for providing soil data, Director of India Meteorological Department (IMD, Pune) for providing rainfall data. Critical and constructive comments from the editor and four anonymous reviewers improved the manuscript significantly.

## References

- Abijith D, Saravanan S, Singh L, Jennifer JJ, Saranya T, Parthasarath KSS (2020) GIS-based multi-criteria analysis for identification of potential groundwater recharge zones—a case study from Pon-naniyaru watershed, Tamil Nadu, India. *HydroResearch* 3:1–14. <https://doi.org/10.1016/j.hydres.2020.02.002>
- Adeyeye OA, Ikpokonte EA, Arabi SA (2019) GIS-based groundwater potential mapping within Dengi area, North Central Nigeria. *Egypt J Remote Sens Space Sci* 22:175–181. <https://doi.org/10.1016/j.ejrs.2018.04.003>
- Ahmed R, Sajjad H (2018) Analyzing factors of groundwater potential and its relation with population in the lower Barpani Watershed, Assam India. *Nat Resour Res*. <https://doi.org/10.1007/s11053-017-9367-y>
- Al-Abadi AM (2017) Modelling of groundwater productivity in north-eastern Wasit Governorate, Iran using frequency ratio and Shannon's entropy models. *Appl Water Sci* 7:699–716. <https://doi.org/10.1007/s13201-015-0283-1>
- Al-Abadi AM, Al-Temmeme AA, Al-Ghanimy MA (2016) A GIS-based combining of frequency ratio and index of entropy approaches for mapping groundwater availability zones at Badra-Al Al-Gharbi-Teeb areas, Iraq. *Sustain Water Resour Manag* 2:265–283. <https://doi.org/10.1007/s40899-016-0056-5>
- Andualem TG, Demeke GG (2019) Groundwater potential assessment using GIS and remote sensing: a case study of Guna tana landscape, upper blue Nile Basin. *Ethiopia J Hydrol Reg Stud* 24:100610. <https://doi.org/10.1016/j.ejrh.2019.100610>
- Arabameri A, Rezaei K, Cerda A, Lombardo L, Rodrigo-Comino J (2019) GIS-based groundwater potential mapping in Shahroud plain, Iran. A comparison among statistical (bivariate and multivariate), data mining and MCDM approaches. *Sci Total Environ* 658:160–177. <https://doi.org/10.1016/j.scitotenv.2018.12.115>
- Bagyaraj M, Ramkumar T, Venkatramanan S, Gurugnanam B (2013) Application of remote sensing and GIS analysis for identifying groundwater potential zone in parts of Kodaikanal Taluk, South India. *Front Earth Sci* 7(1):65–75. <https://doi.org/10.1007/s11707-012-0347-6>
- Balamurugan G, Seshan K, Bera S (2017) Frequency ratio model for groundwater potential mapping and its sustainable management in cold desert, India. *J King Saud Univ Sci* 29:333–347. <https://doi.org/10.1016/j.jksus.2016.08.003>
- Benaafi M, Hariri M, Abdullatif O, Makkawi M, Al-Shaibani A (2017) Analysis of lineaments within the Wajid group, SW Saudi Arabia, and their tectonic significance. *Arab J Geosci* 10:106. <https://doi.org/10.1007/s12517-017-2860-0>
- Berhanu KG, Hatiye SD (2020) Identification of groundwater potential zones using proxy data: case study of Megech Watershed. *Ethiopia J Hydrol Reg Stud* 28:100676. <https://doi.org/10.1016/j.ejrh.2020.100676>
- Bonham-Carter GF (1994) Geographic information systems for geoscientists: modeling with GIS. Pergamon Press, Ottawa
- Bui DT, Pradhan B, Lofman O, Revhaug I, Dick OB (2011) Landslide susceptibility mapping at Hoa Binh Province (Vietnam) using an adaptive neuro-fuzzy inference system and GIS. *Comput Geosci*. <https://doi.org/10.1016/j.cageo.2011.10.031>
- CGWB (2012) Dynamic Ground Water Resources of India (as on March 2019). Central Ground Water Board (CGWB), New Delhi
- Chen W, Li H, Hou E, Wang S, Wang G, Panahi M, Li T, Peng T, Guo C, Niu C, Xiao L, Wang J, Xie X, Ahmad B (2018) GIS-based groundwater potential analysis using novel ensemble weights-of-evidence with logistic regression and functional tree models. *Sci Total Environ* 634:853–867. <https://doi.org/10.1016/j.scitotenv.2018.04.055>
- Chow VT (1964) Handbook of applied hydrology. McGraw Hill Inc, New York
- Das S (2018a) Geomorphic characteristics of a bedrock river inferred from drainage quantification, longitudinal profile, knickzone identification and concavity analysis: a DEM-based study. *Arab J Geosci* 11:680. <https://doi.org/10.1007/s12517-018-4039-8>
- Das S (2018b) Geographic information system and AHP-based flood hazard zonation of Vaitarna basin, Maharashtra, India. *Arab J Geosci* 11:576. <https://doi.org/10.1007/s12517-018-3933-4>
- Das S (2019a) Four decades of water and sediment discharge records in Subarnarekha and Burhabalang basins: an approach towards trend analysis and abrupt change detection. *Sustain Water Resour Manag* 5:1665–1676. <https://doi.org/10.1007/s40899-019-00326-1>
- Das S (2019b) Comparison among influencing factor, frequency ratio, and analytical hierarchy process techniques for groundwater potential zonation in Vaitarna basin, Maharashtra, India. *Groundw Sustain Dev* 8:617–629. <https://doi.org/10.1016/j.gsd.2019.03.003>
- Das S (2019c) Geospatial mapping of flood susceptibility and hydrogeomorphic response to the floods in Ulhas basin, India. *Remote*

- Sens Appl Soc Environ 14:60–74. <https://doi.org/10.1016/j.rsase.2019.02.006>
- Das S (2020) Landscape variables in the Indian (Peninsular) catchments: insights into hydro-geomorphic evolution. *Earth*. <https://doi.org/10.31223/osf.io/hbsq2>
- Das S, Pardeshi SD (2018a) Morphometric analysis of Vaitarna and Ulhas river basins, Maharashtra, India: using geospatial techniques. *Appl Water Sci* 8:158. <https://doi.org/10.1007/s13201-018-0801-z>
- Das S, Pardeshi SD (2018b) Comparative analysis of lineaments extracted from Cartosat, SRTM and Aster DEM: a study based on four watersheds in Konkan region, India. *Spat Inf Res* 26(1):47–57. <https://doi.org/10.1007/s41324-017-0155-x>
- Das S, Pardeshi SD (2018c) Integration of different influencing factors in GIS to delineate groundwater potential areas using IF and FR techniques: a study of Pravara basin, Maharashtra, India. *Appl Water Sci* 8:197. <https://doi.org/10.1007/s13201-018-0848-x>
- Das S, Gupta A, Ghosh S (2017) Exploring groundwater potential zones using MIF technique in semi-arid region: a case study of Hingoli district, Maharashtra. *Spat Inf Res* 25(6):749–756. <https://doi.org/10.1007/s41324-017-0144-0>
- Das S, Pardeshi SD, Kulkarni PP, Doke A (2018) Extraction of lineaments from different azimuth angles using geospatial techniques: a case study of Pravara basin, Maharashtra, India. *Arab J Geosci* 11:160. <https://doi.org/10.1007/s12517-018-3522-6>
- Doke A (2019) Delineation of the groundwater potential using remote sensing and GIS: a case study of Ulhas basin, Maharashtra, India. *Arch Photogramm Cartogr Remote Sens* 31:49–64. <https://doi.org/10.2478/apcrs-2019-0004>
- Doke A, Pardeshi SD, Pardeshi SS, Das S (2018) Identification of morphogenetic regions and respective geomorphic processes: a GIS approach. *Arab J Geosci* 11:20. <https://doi.org/10.1007/s12517-017-3358-5>
- Etikala B, Golla V, Li P, Renati S (2019) Deciphering groundwater potential zones using MIF technique and GIS: a study from Tirupati area, Chittoor District, Andhra Pradesh, India. *HydroResearch* 1:1–7. <https://doi.org/10.1016/j.hydres.2019.04.001>
- Farr TG, Kobrick M (2000) Shuttle radar topography mission produces a wealth of data. *Am Geophys Union, EOS* 81:583–585. <https://doi.org/10.1029/EO081i048p00583>
- Ganapuram S, Kumar GTV, Krishna IVM, Kahya E, Demirel MC (2009) Mapping of groundwater potential zones in the Musi basin using remote sensing data and GIS. *Adv Eng Softw* 40:506–518. <https://doi.org/10.1016/j.advengsoft.2008.10.001>
- Ghasemlounia R, Herfeh NS (2017) Study on groundwater quality using geographic information system (GIS), case study: Ardabil. *Iran Civil Eng J* 3:779–793. <https://doi.org/10.21859/cej-030914>
- Gnanachandrasamy G, Zhou Y, Bagyaraj M, Venkatramanan S, Ramkumar T, Wang S (2018) Remote sensing and GIS based groundwater potential zone mapping in Ariyalur District, Tamil Nadu. *J Geol Soc India* 92:484–490. <https://doi.org/10.1007/s12594-018-1046-z>
- Grohmann CH (2004) Morphometric analysis in geographic information systems: applications of free software GRASS and R. *Comput Geosci* 30:1055–1067. <https://doi.org/10.1016/j.cageo.2004.08.002>
- Hadley RF, Schumm SA (1961) Sediment sources and drainage basin characteristics in upper Cheyenne River Basin. *US Geol Surv Water Supply Pap* 1531:198
- Horton RE (1932) Drainage basin characteristics. *Trans Am Geophys Union* 13:350–361. <https://doi.org/10.1029/TR013i001p00350>
- Horton RE (1945) Erosional development of streams and their drainage basins: hydrophysical approach to quantitative morphology. *Bull Geol Soc Am* 56:275–370. [https://doi.org/10.1130/0016-7606\(1945\)56\[275:EDOSAT\]2.0.CO;2](https://doi.org/10.1130/0016-7606(1945)56[275:EDOSAT]2.0.CO;2)
- Hosseini M, Saremi A (2018) Assessment and estimating groundwater vulnerability to pollution using a modified drastic and gods models (case study: malayer plain of Iran). *Civil Eng J* 4:433–442. <https://doi.org/10.28991/cej-0309103>
- Jenifer MA, Jha MK (2017) Comparison of analytic hierarchy process, catastrophe and entropy techniques for evaluating groundwater prospect of hard-rock aquifer systems. *J Hydrol* 548:605–624. <https://doi.org/10.1016/j.jhydrol.2017.03.023>
- Kanagaraj G, Suganthi S, Elango L, Magesh NS (2019) Assessment of groundwater potential zones in Vellore district, Tamil Nadu, India using geospatial techniques. *Earth Sci Inf* 12:211–223. <https://doi.org/10.1007/s12145-018-0363-5>
- Kumar A, Pandey AC (2016) Geoinformatics based groundwater potential assessment in hard rock terrain of Ranchi urban environment, Jharkhand state (India) using MCDM–AHP techniques. *Groundw Sustain Dev* 2(3):27–34. <https://doi.org/10.1016/j.gsd.2016.05.001>
- Kumar VA, Mondal NC, Ahmed S (2020) Identification of groundwater potential zones using RS, GIS and AHP techniques: a case study in a part of Deccan Volcanic Province (DVP), Maharashtra, India. *J Indian Soc Remote Sens* 48(3):497–511. <https://doi.org/10.1007/s12524-019-01086-3>
- Magesh NS, Chandrasekar N, Soundranayagam JP (2012) Delineation of groundwater potential zones in Theni district, Tamil Nadu, using remote sensing, GIS and MIF techniques. *Geosci Front* 3(2):189–196. <https://doi.org/10.1016/j.gsf.2011.10.007>
- Mahato S, Pal S (2019) Groundwater potential mapping in a rural river basin by union (OR) and intersection (AND) of four multi-criteria decision-making models. *Nat Resour Res*. <https://doi.org/10.1007/s11053-018-9404-5>
- Manap MA, Nampak H, Pradhan B, Lee S, Sulalman WNA, Ramli MF (2014) Application of probabilistic-based frequency ratio model in groundwater potential mapping using remote sensing data and GIS. *Arab J Geosci* 7:711–724. <https://doi.org/10.1007/s12517-012-0795-z>
- Marghany M (2012) Fuzzy B-spline algorithm for 3-D lineament reconstruction. *Int J Phys Sci* 7(15):2294–2301. <https://doi.org/10.5897/IJPS11.1715>
- Mishra A, Dubey DP, Tiwari RN (2011) Morphometric analysis of Tons basin, Rewa District, Madhya Pradesh, based on watershed approach. *Earth Sci India* 4:171–180
- Misi A, Gumindoga W, Hoko Z (2018) An assessment of groundwater potential and vulnerability in the Upper Manyame Sub-Catchment of Zimbabwe. *Phys Chem Earth* 105:72–83. <https://doi.org/10.1016/j.pce.2018.03.003>
- Mokadem N, Boughariou E, Mudarra M, Brahim FB, Andreo B, Hamed Y, Bouri S (2018) Mapping potential zones for groundwater recharge and its evaluation in arid environments using a GIS approach: case study of North Gafsa Basin (Central Tunisia). *J Afr Earth Sci* 141:107–117. <https://doi.org/10.1016/j.jafrearsci.2018.02.007>
- Nigussie W, Hailu BT, Azagegn T (2019) Mapping of groundwater potential zones using sentinel satellites (–1 SAR and –2A MSI) images and analytical hierarchy process in Ketar watershed, Main Ethiopian Rift. *J Afr Earth Sci* 160:103632. <https://doi.org/10.1016/j.jafrearsci.2019.103632>
- Nithya CN, Srinivas Y, Magesh NS, Kaliraj S (2019) Assessment of groundwater potential zones in Chittar basin, Southern India using GIS based AHP technique. *Remote Sens Appl Soc Environ* 15:100248. <https://doi.org/10.1016/j.rsase.2019.100248>
- Nsiah E, Appiah-Adjei EK, Adjei KA (2018) Hydrogeological delineation of groundwater potential zones in the Nabogo basin, Ghana. *J Afr Earth Sci* 143:1–9. <https://doi.org/10.1016/j.jafrearsci.2018.03.016>
- Pal S, Kundu S, Mahato S (2020) Groundwater potential zones for sustainable management plans in a river basin of India and



- Bangladesh. *J Clean Prod* 257:120311. <https://doi.org/10.1016/j.jclepro.2020.120311>
- Pande CB, Moharir KN, Singh SK, Varade AN (2019) An integrated approach to delineate the groundwater potential zones in Devdari watershed area of Akola district, Maharashtra, Central India. *Environ Dev Sustain* 3:1–21. <https://doi.org/10.1007/s10668-019-00409-1>
- Pandey PK, Das SS (2016) Morphometric analysis of Usri river basin, Chhotanagpur plateau, India, using remote sensing and GIS. *Arab J Geosci* 9:240. <https://doi.org/10.1007/s12517-015-2287-4>
- Patra S, Mishra P, Mahapatra SC (2018) Delineation of groundwater potential zone for sustainable development: a case study from Ganga Alluvial Plain covering Hooghly district of India using remote sensing, geographic information system and analytic hierarchy process. *J Clean Prod* 172:2485–2502. <https://doi.org/10.1016/j.jclepro.2017.11.161>
- Pham BT, Jaafari A, Prakash I, Singh SK, Quoc NK, Bui DT (2019) Hybrid computational intelligence models for groundwater potential mapping. *CATENA* 182:104101. <https://doi.org/10.1016/j.catena.2019.104101>
- Pham BT, Avand M, Janizadeh S, Phong TV, Al-Ansari N, Ho LS, Das S, Le HV, Amini A, Bozchaloei SK, Jafari F, Prakash I (2020) GIS based hybrid computational approaches for flash flood susceptibility assessment. *Water* 12:683. <https://doi.org/10.3390/w12030683>
- Pike RJ, Wilson SE (1971) Elevation-relief ratio, hypsometric integral, and geomorphic area altitude analysis. *Geol Soc Am Bull* 82:1079–1084. [https://doi.org/10.1130/0016-7606\(1971\)82\[1079:ERHIAG\]2.0.CO;2](https://doi.org/10.1130/0016-7606(1971)82[1079:ERHIAG]2.0.CO;2)
- Pradhan B, Lee S (2010) Landslide susceptibility assessment and factor effect analysis: backpropagation artificial neural networks and their comparison with frequency ratio and bivariate logistic regression modelling. *Environ Modell Softw* 25:747–759. <https://doi.org/10.1016/j.envsoft.2009.10.016>
- Preeja KR, Sabu J, Thomas J, Vijith H (2011) Identification of groundwater potential zones of a tropical river basin (Kerala, India) using remote sensing and GIS techniques. *J Indian Soc Remote Sens* 39(1):83–94. <https://doi.org/10.1007/s12524-011-0075-5>
- Raju RS, Raju GS, Rajasekhar M (2019) Identification of groundwater potential zones in Mandavi River basin, Andhra Pradesh, India using remote sensing, GIS and MIF techniques. *HydroResearch* 2:1–11. <https://doi.org/10.1016/j.hydres.2019.09.001>
- Rao NS (2006) Groundwater potential index in a crystalline terrain using remote sensing data. *Environ Geol* 50:1067–1076. <https://doi.org/10.1007/s00254-006-0280-7>
- Rizeei HM, Pradhan B, Saharkhiz MA, Lee S (2019) Groundwater aquifer potential modeling using an ensemble multi-adoptive boosting logistic regression technique. *J Hydrol* 579:124172. <https://doi.org/10.1016/j.jhydrol.2019.124172>
- Rodell M, Velicogna I, Famiglietti JS (2009) Satellite-based estimates of groundwater depletion in India. *Nature* 460(7258):999–1002. <https://doi.org/10.1038/nature08238>
- Schumm SA (1956) Evolution of drainage systems and slopes in bad lands at Perth Amboy, New Jersey. *Bull Geol Soc Am* 67:597–646
- Schumm SA (1963) Sinuosity of alluvial rivers in the great plains. *Bull Geol Soc Am* 74:1089–1100. [https://doi.org/10.1130/0016-7606\(1963\)74\[1089:SOAROT\]2.0.CO;2](https://doi.org/10.1130/0016-7606(1963)74[1089:SOAROT]2.0.CO;2)
- Smith KG (1950) Standards for grading texture of erosional topography. *Am J Sci* 248:655–668. <https://doi.org/10.2475/ajs.248.9.655>
- Sreedevi PD, Owais S, Khan HH, Ahmed S (2009) Morphometric analysis of a watershed of South India using SRTM data and GIS. *J Geol Soc India* 73:543–552. <https://doi.org/10.1007/s12594-009-0038-4>
- Strahler AN (1957) Quantitative analysis of watershed geomorphology. *Trans Am Geophys Union* 38:913–920. <https://doi.org/10.1029/TR038i006p00913>
- Strahler AN (1964) Quantitative geomorphology of drainage basins and channel networks. In: Chow VT (ed) *Hand book of applied hydrology*. McGraw Hill Book Company, New York
- Thapa R, Gupta S, Guni S, Kaur H (2017) Assessment of groundwater potential zones using multi-influencing factor (MIF) and GIS: a case study from Birbhum district, West Bengal. *Appl Water Sci* 7:4117–4131. <https://doi.org/10.1007/s13201-017-0571-z>
- Thomas R, Duraisamy V (2017) Hydrological delineation of groundwater vulnerability of droughts in semi-arid areas of western Ahmednagar district. *Egypt J Remote Sens Space Sci*. <https://doi.org/10.1016/j.ejrs.2016.11.008>
- Venkateswarana S, Ayyanduraib R (2015) Groundwater potential zoning in Upper Gadilam River Basin, Tamil Nadu. *Aquat Proc* 4:1275–1282. <https://doi.org/10.1016/j.aqpro.2015.02.166>
- Widdowson M, Cox KG (1996) Uplift and erosional history of the Deccan Traps, India: evidence from laterites and drainage patterns of the Western Ghats and Konkan Coast. *Earth Planet Sci Lett* 137:57–69. [https://doi.org/10.1016/0012-821X\(95\)00211-T](https://doi.org/10.1016/0012-821X(95)00211-T)
- Wood WF, Snell JB (1960) A Quantitative System for Classifying Landforms. In: *Quartermaster research and engineering command, US Army technical report, EP-124*
- Yeh H-F, Cheng Y-S, Lin H-I, Lee C-H (2016) Mapping groundwater recharge potential zone using a GIS approach in Hualian River, Taiwan. *Sustain Environ Res* 26:33–43. <https://doi.org/10.1016/j.serj.2015.09.005>
- Yousef AH, Prijub CP, Prasadb NBN (2015) Delineation of groundwater potential zones in deep midland aquifers along Bharathapuzha River Basin Kerala using geophysical methods. *Aquat Proc* 4:1039–1046. <https://doi.org/10.1016/j.aqpro.2015.02.131>
- Zaidi FK (2011) Drainage basin morphometry for identifying zones for artificial recharge: a case study from Gagas river basin, India. *J Geol Soc India* 77:160–166. <https://doi.org/10.1007/s12594-011-0019-2>

**Publisher's Note** Springer Nature remains neutral with regard to jurisdictional claims in published maps and institutional affiliations.

Reproduced with permission of copyright owner. Further reproduction prohibited without permission.